Available online at www.springerlink.com

Acta Metall. Sin. (Engl. Lett.) Vol.26 No. 5 pp. 630—634 October 2013

ACTA
METALLURGICA SINICA
(ENGLISH LETTERS)

Electrical Properties and Local Domain Structure of $LiNbO_3$ Thin Film Grown by Ion Beam Sputtering Method

V. Ievlev[1)], *V. Shur*[2)], *M. Sumets*[1,3)†] *and A. Kostyuchenko*[1)]

1) Voronezh State University, Universitetskaya Square, 1, 394000, Voronezh, Russia

2) Ferroelectric Laboratory IPAM, Ural State University, pr. Lenina, 51, 620083, Ekaterinburg, Russia

3) Voronezh Institute of the State Fire Service of Russian Emergencies Ministry, Krasnoznamennaya st., 231, 394052, Voronezh, Russia

[Manuscript received 16 January 2012, in revised form 16 April 2013]

The nanocrystalline ferroelectric $LiNbO_3$ films on (001) Si substrates with the random orientation of polycrystalline grains and the predominance of the grains with lateral orientation of the polar axis were grown using the ion beam sputtering method. The remanent polarization and the coercive field are 12 $\mu C/cm^2$ and 29 kV/cm, respectively. The thermal annealing leads to the coarsening of the grains. The appearance of the "local texture," which gives rise to the unipolarity of the heterostructures caused by the predominance of the one direction in the vertical component of the spontaneous polarization, is investigated.

KEY WORDS: $LiNbO_3$ thin films; Ferroelectrics; Domain structure

1. Introduction

Lithium niobate is the promising material to create the memory units, electrooptical devices, and waveguides. To develop the elements of integral optics, the thin $LiNbO_3$ films with predetermined properties are required. Two of the effective methods of thin film growing with no changes in their elemental composition are RF magnetron sputtering and ion beam sputtering (IBS)[1−4]. These methods can be used to create a wide range of integrated elements such as optical and acoustic wave conductors and light-emitting diodes[5−7]. It is generally accepted that the development of the technological regimes is a main step during the sputtering process because they allow the creation of active layers not only with well-controlled structural properties but also with desired electrical, spectral, and optical parameters. Nevertheless, despite the thin films of $LiNbO_3$ being important elements because of relatively wide scope of their possible practical applications, some crucial properties of the films and interface film-substrate playing an important role in the device′s work still have not been studied thoroughly. For example, this is a well-known fact that the structure of the $LiNbO_3$ films largely influences their electrical properties, and the local domain structure is the main factor for the domain kinetics in ferroelectrics and, as a result, controls the processes of the polarization switching[8,9]. Moreover, some investigators[10,11] reported that several important parameters of the ferroelectric films, such as remanent polarization and coercive field derived from the dielectric-hysteresis loops, are affected by the local domain structure and non-switchable "passive layers" and other factors originating from the texture and crystalline orientation of $LiNbO_3$ material. It is important to emphasize that relaxation phenomena underlie many electrical properties of the ferroelectric film and can even block switching process, which is the stumbling block of the contemporary electronics. From this point of view, various approaches, such as optimization of the sputtering parameters[12], doping[13] and annealing[14] have been applied to obtain the desired result in switching of the ferroelectric devices. Consequently, there is no doubt that investigation of the relation between the structure of the grown films and their relaxation properties is urgent. The present paper aims to study the relaxation prop-

† Corresponding author. Tel.: +7 906-590-04-65; E-mail address: maxsumets@gmail.com (M. Sumets)

DOI: 10.1007/s40195-013-0025-z

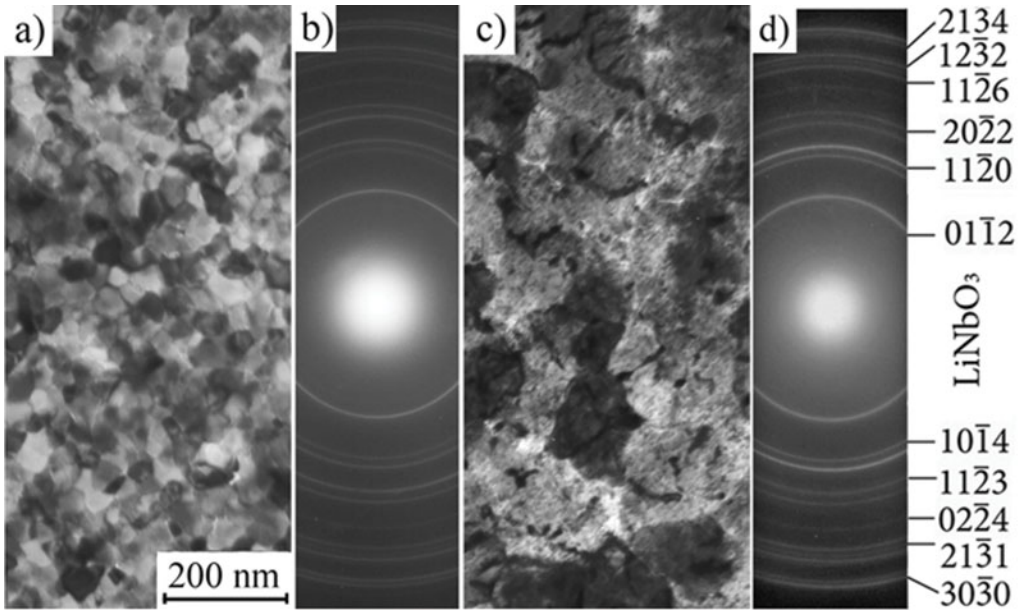

Fig. 1 Micrographs and electron diffraction patterns of $LiNbO_3$ films with thickness of about 0.1 μm, grown on the heated (550 °C) (001)Si substrate by the ion-beam sputtering method: (a, b) as-grown; (c, d) after thermal annealing at 700 °C for 60 min

erties of thin $LiNbO_3$ film grown by the ion beam sputtering method, as well as their local domain structure and subsequent thermal annealing effect.

2. Experimental

The films with thickness up to 1.0 μm were obtained in the IBS process. The sputtering was conducted in Ar environment (0.1 Pa) with the use of a 2 kW power supply. The film growth rate was approximately 3 nm/min. The distance between the target and the bottom layer about 4.0–5.0 cm. Wafers of monocrystalline silicon of (001) orientation, with n-type of conductivity and specific resistance of 4.5 Ω·cm, were used as substrates. The subsequent annealing of the heterostructures was conducted for 60 min in air environment at 650 °C.

The study of the structure was conducted by transmission electron microscopy (EMV-100BR). The electrical properties of (001)Si-$LiNbO_3$ heterostructures were investigated using impedance spectroscopy. Impedance was obtained with the use of the impedance analyzer "Solartron 1260" at 25 °C. The top contacts for the electrical measurements having area S=5×10^{-6} m^2 were formed by thermal evaporation and condensation of Al in vacuum (1×10^{-4} Pa). The ferroelectric properties were studied by recording of the hysteresis loops and by visualization of the domain structure by piezoresponse force microscopy (PFM) using scanning probe laboratory NTEGRA-Aura (NT MDT, Russia). All details concerning the experimental methodology and interpretation of the results in the framework of PFM method are quite well known and can be found in Ref. [15].

3. Results and Discussion

3.1 Structure

It has been established by the transmission electron microscopy (TEM) that the nanocrystalline films are formed on the (001)Si substrate at 550 °C in the process of ion beam sputtering. Fig. 1(a) and Fig. 1(b) show the micrograph and electron diffraction pattern of the film with width 0.1 μm grown on the heated (001)Si substrate. Analysis by electron diffraction shows that the single-phase $LiNbO_3$ film-swith random orientation of the grains is formed. The grain size does not exceed 50 nm.

Recrystallization of the film and formation of the block crystalline substructure (block size less than 200 nm), consisting of $LiNbO_3$ subgrains (the average size is about 80 nm) (Fig. 1(c) and Fig. 1(d)), occur as a result of thermal annealing of the heterostructure (001) Si–nanocrystalline film $LiNbO_3$.

3.2 Impedance spectroscopy

Impedance spectroscopy is widely used to study relaxation processes in the thin film. Usually, two types of plots are used to represent the experimental results, include complex plane (Nyquist plots) and Bode plots. The complex plane plot is a plot of Z'' *vs.* Z', that is, the imaginary *vs.* the real components, plotted for various frequencies, ω. The other types of graphs are Bode plots, that is, lg|Z| (magnitude) *vs.* lgω, and phase-angle, φ *vs.* lgω. The Nyquist and Bode diagrams for as-grown (100)Si-$LiNbO_3$ heterostructures and for structures after thermal anneal-

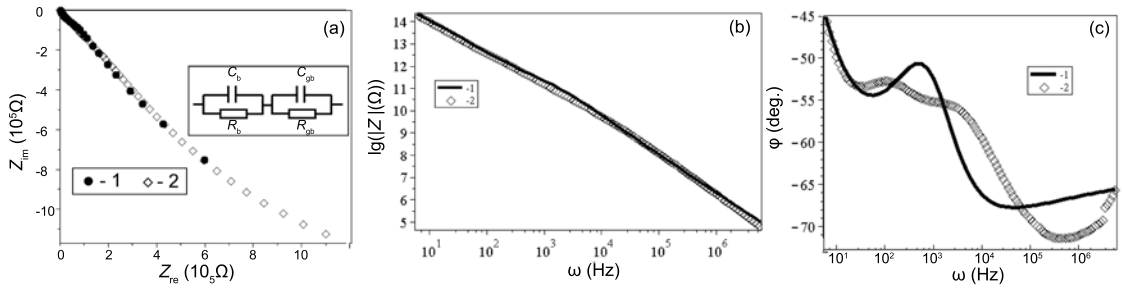

Fig. 2 Diagrams of Nyquist (a), lg|Z| *vs.* lgω (b) and φ *vs.* lgω (c) of as-grown (001)Si-$LiNbO_3$ heterostructures (c) (1–calculated by Eq. (1); 2–experimental)

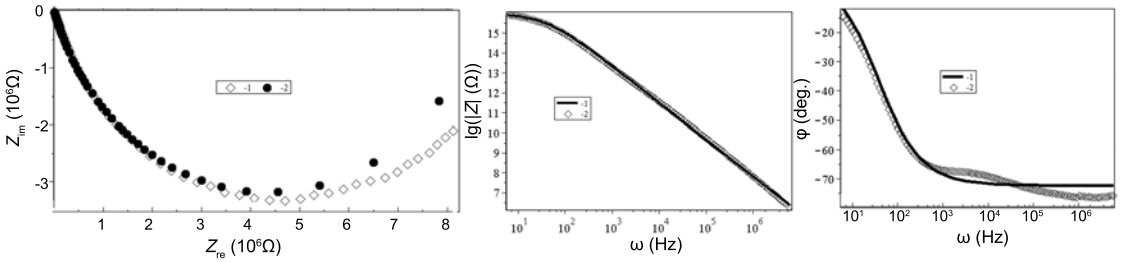

Fig. 3 Diagrams of Nyquist (a), lg|Z| *vs.* lgω (b) and φ *vs.* lgω (c) of (001)Si-$LiNbO_3$ heterostructures after thermal annealing (1–calculated by Eq. (1); 2–experimental)

Table 1 Analysis results for Nyquist and Bode diagrams

Structure type	R_{gb} (Ω)	C_{gb} (F)	τ_1 (s)	α_1	R_b (Ω)	C_b (F)	τ_2 (s)	α_2
As-grown	5×10^6	1.2×10^{-7}	0.6	0.3	4×10^4	7×10^{-8}	3×10^{-4}	0.1
After thermal annealing	8.7×10^6	3×10^{-9}	2.6×10^{-2}	0.2	–	–	–	–

ing, grown by IBS method, are presented in Fig. 2 and Fig. 3. With the approach presented in Ref. [16] where it has been emphasized that electrical properties of the (001)Si-$LiNbO_3$ heterostructures largely depend on the $LiNbO_3$ layer as our basis, we have described the impedance spectra using the electrical equivalent circuit shown in Fig. 2(a) (see insert). Here, R_{gb}, C_{gb}, and R_b, C_b are the resistance and capacitance of the grain boundary and the grain, respectively. In this case, the complex impedance for such circuit is as follows:

$$Z^* = \frac{R_b}{1+(j\omega\tau_1)^{1-\alpha_1}} + \frac{R_{gb}}{1+(j\omega\tau_2)^{1-\alpha_2}}$$

were, $\tau_1 = R_bC_b$ and $\tau_2 = R_{gb}C_{gb}$ are the characteristic times of the corresponding relaxation process, j is the imaginary unit, α_i is the coefficient describing the width of the relaxation time distribution spectrum ($0 \le \alpha_i \le 1$). The analysis of the results obtained through the fitting of the experimental data and the theoretical calculation results obtained from Eq. (1) are shown in Table 1.

It is seen from Table 1 that the thermal annealing leads to a decrease in the relaxation time of the "slow" relaxation process, which seems to be conditioned by the influence of the grain boundaries in the $LiNbO_3$ film. As it has been proposed[12], vacancies appearing inevitably in the $LiNbO_3$ film during the growing process play a crucial role in the relaxation process. For example, the oxygen vacancies (positive charges) may have originated from the sputtering process of the film and can be associated with bulk properties of the film. On the other hand, negative charges could be induced by the presence of negative charged oxygen trapped at the grain boundaries, and apparently, thermal annealing affects (decreases) oxygen concentration considerably. In any case, this issue is not clear, and it is necessary to carry out a more intensive study.

3.3 Polarization hysteresis and local domain structure

Fig. 4 shows the hysteresis loops of the as-grown (100)Si-$LiNbO_3$heterostructures and the heterostructures after thermal annealing. It can be shown that all films are ferroelectric ones. Besides the values of remanent polarization P_r, coercive field E_c and internal field $E_i = (E_c^+ + E_c^-)/2$ derived from Fig. 4 are presented in Table 2.

It follows from Table 2 that thermal annealing leads to decline in the value of remanent polarization and causes appearance of the pretty high E_i. Moreover, it can be clearly seen that thermal annealing of the (100)Si-$LiNbO_3$ heterostructures triggers the displacement of the hysteresis loops along the vertical

Table 2 Parameters of dielectric loops of the (001)Si-$LiNbO_3$ heterostructurespar

Type of heterostructure	P_r^+ ($\mu C/cm^2$)	P_r^- ($\mu C/cm^2$)	E_c^+ (kV/cm)	E_c^- (kV/cm)	E_i (kV/cm)
As-grown	11.2	−12.4	29	−29	0
After thermal annealing	−6.4	−10	28	78	53

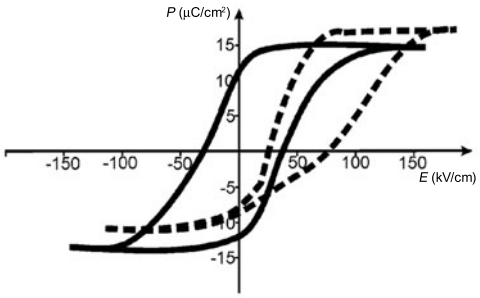

Fig. 4 Dielectric-hysteresis loops of (001)Si-$LiNbO_3$ heterostructures (sold line – as-grown; dotted line – after thermal annealing)

axis, which may prove unipolarity of the studied structures. To investigate the reason for this shift, we have carried out a research of the local domain structure of $LiNbO_3$ films through visualization of the domain structure by the AFM and PFM.

In the present work, two components of the spontaneous polarization, vertical and horizontal ones lying along the film′s surface, have been studied. Fig. 5 shows the AFM and PFM images of the as-grown $LiNbO_3$ film. In Fig. 5(a), the structure with the average grain size of 250 nm is clearly seen. In Fig. 5(b), for the signal of vertical piezoresponse, three contrasts that light, dark and intermediate are observed. The light and the dark contrasts correspond to the domains with the predominantly vertical polarization direction, which are different in the direction (up or down). The intermediate contrast corresponds to the polarization direction, lying predominantly in the plane of the specimen surface. Thus, the analysis of the data in Fig. 5 has shown that in the as-grown $LiNbO_3$ film, the polar axes in the grains have random orientation with the predominance of the grains with the lateral orientation of the polar axis. Fig. 6(a) clearly shows that one direction of the vertical component polarization is predominant to compare with

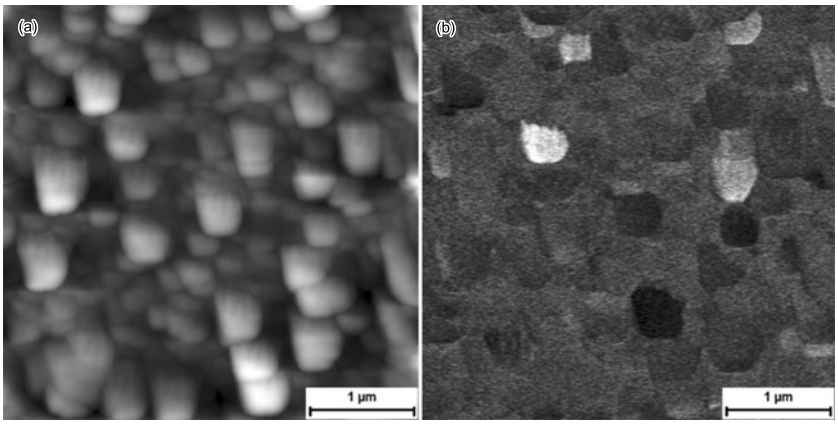

Fig. 5 AFM image (a) and PFM image (the vertical component) (b) of as-grown $LiNbO_3$ film

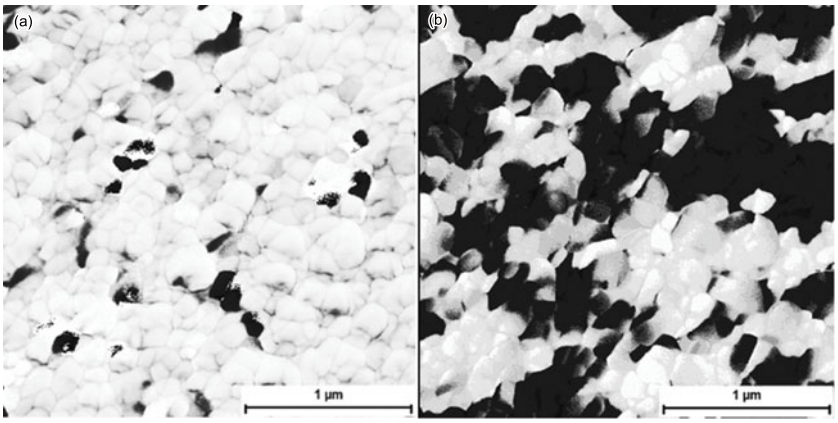

Fig. 6 PFM images of the annealed $LiNbO_3$ film: (a) vertical component; (b) lateral component

another one; therefore, this fact indicates that in our case, thermal annealing of the (100)Si-$LiNbO_3$ heterostructures leads to the occurrence of the "local texture," that is, the areas with preferred domain orientation. As far as the lateral component is concerned, the complex domain structure is observed (Fig. 6(b)). This fact indicates that after thermal annealing, the polar axis directions, lying neither in the surface plane nor normal to it, predominate in the $LiNbO_3$ film. Regretfully, the experiments on the local switching for as-grown $LiNbO_3$ film and for the film after thermal annealing (at the voltage up to 50 V) yielded no results, which may be due to the random orientation of the polar axis in the grains. However, the occurrence of the "local texture" with the predominance of one direction for the vertical component of spontaneous polarization in the $LiNbO_3$ films after thermal annealing is in a good agreement to the shift of the hysteresis loops described previously, which is suggestive of the unipolarity in the studied film.

4. Conclusion

During the ion-sputtering process, the $LiNbO_3$ polycrystalline films with random grain orientation are formed on the (001)Si substrates. Two relaxation processes with the relaxation time τ_1=0.6 s and $\tau_2=3\times10^{-4}$ s were revealed using the impedance spectroscopy. The first process ("slow") seems to be due to the grain boundary properties and the second one ("rapid") to their bulk properties. The film manifested the ferroelectric properties; the values of the remanent polarization and the coercive field were equal to P_r=12 μC/cm^2 and E_c=29 kV/cm, respectively. The investigation of the local domain structure demonstrated that, in the as-grown $LiNbO_3$ film, the polar axes of the grains are random oriented ones, with the grains with the lateral axis orientation predominating. The thermal annealing of the films at 650 °C leads to the decrease in the relaxation time for the "slow" process and disappearance of the "rapid" one, which is suggestive of the predominant influence of the grain boundaries on electrical properties of the (100)Si-$LiNbO_3$ heterostructures. The change of the local domain structure of $LiNbO_3$ film after thermal annealing is revealed in the occurrence of the "local texture," *i.e.*, the areas with the tens of the grains with the same direction of the polar axis. The lateral component of the spontaneous polarization has the complex structure and lies neither in the film plane nor normal to it. It should be noted that in the $LiNbO_3$ film after thermal annealing, the predominance of one direction of the vertical component of spontaneous polarization is observed, which accounts for the shift of the hysteresis loops along the vertical axis. There is no doubt that this phenomenon demands to be studied more intensively in our further research study.

REFERENCES

[1] K. Benaissa, P.V. Ashrit, G. Bader, F.E. Girouard and V.V. Truong, Thin Solid Films **214** (1992) 219.
[2] T.H. Lee, F.T. Hwang, C.T. Lee and H.Y. Lee, Mater. Sci. Eng. **136** (2007) 92.
[3] V. Iyevlev, A. Kostyuchenko and M. Sumets, in: Proceeding of SPIE to the 16th International School on Quantum Electronics: Laser Physics and Applications, Nessebar, Bulgaria, September 20, 2010.
[4] V.M. Ievlev, M.P. Sumets and A.V. Kostyuchenko, Mater. Sci. Forum **700** (2012) 53.
[5] Z. Zang, T. Minato, P. Navaretti, Y. Hinokuma, M. Duelk, C. Velez and K. Hamamoto, IEEE Photonics Technol. Lett. **22** (2010) 721.
[6] Z. Zang, K. Mukai, P. Navaretti, M. Duelk, C. Velez and K. Hamamoto, Appl. Phys. Lett. **100** (2012) 031108.
[7] Z. Zang, K. Mukai, P. Navaretti, M. Duelk, C. Velez and K. Hamamoto, IEICE Trans. Electron. **E94-C** (2011) 862.
[8] V. Shur, E. Rumyantsev, R. Batchko, G. Miller, M. Fejer and R. Byer, Ferroelectrics **221** (1999) 157.
[9] V. Ya. Shur, Ferroelectrics **340** (2006) 3.
[10] A. K. Tagantsev and G. Gerra, J. Appl. Phys. **100** (2006) 051607.
[11] V. Edon, D. Re'miens, S. Saada, Appl. Surf. Sci. **256** (2009) 1455.
[12] A.Z. Simões, M.A. Zaghete, B.D. Stojanovic, A.H. Gonzalez, C.S. Riccardi, M. Cantoni and J.A. Varela, J. Eur. Ceram. Soc. **24** (2004) 1607.
[13] C. Nguyen, P. V. Ashrit, G. Bader, F. Girouard and V.V. Truong, J. Appl. Phys. **76** (1994) 4327.
[14] N.S.L.S. Vasconcelos, J.S. Vasconcelos, V. Bouquet, S.M. Zanetti, E.R. Leite, E. Longo, L.E.B. Soledade, F.M. Pontes, M. Guilloux-Viry, A. Perrin, M.I. Bernardi and J.A. Varela, Thin Solid Films **436** (2003) 213.
[15] E. Soergel, J. Phys. D: Appl. Phys. **44** (2011) 464003.
[16] V. Iyevlev, M. Sumets and A. Kostyuchenko, J. Mater. Sci.: Mater. Electron. **23** (2012) 913.